Distant Proximity Orbits About Asteroids

Daniel J. Scheeres

（Smead Aerospace Engineering Sciences Department，University of Colorado Boulder，Boulder 80309-0429，USA）

Abstract： This paper considers the design and dynamics of spacecraft distant from an asteroid， whose gravitational attraction can be neglected at leading order. The motion of the spacecraft then is a function of solar gravity and solar radiation pressure. The differential acceleration between the spacecraft and the small asteroid creates a unique relative dynamics between the two bodies， and provides the spacecraft certain orbits that will remain in the vicinity of the asteroid and which could be used advantageously for observations. The current paper completely solves the simpler case when the asteroid is in a circular heliocentric orbit. The elliptic case is also considered and formulated， with some initial results identified.

Keywords： asteroid；proximity orbit；motion equation；higher order corrections

Highights：

- Relative motion about small asteroids will be dominated by the satellite dynamics relative to the asteroid's heliocentric orbit.
- Relative heliocentric orbits are strongly affected by the asteroid orbits eccentricity，but can be analyzed using the Tschauner-Hempel equations.
- Specific mission designs and initial orbit conditions are defined for trajectories which stay bound to the asteroid.

Introduction

Spacecraft missions to asteroids are a topic of great interest for the scientific and engineering communities. They are the most accessible planetary bodies outside of the Earth-Moon system, their study can deepen our scientific understanding of the formation circumstances of the solar system, and in the future they may prove to be key elements of the exploration infrastructure due to their mineral composition. They also can prove hazardous to society, as the impact of an asteroid could create significant damage on the surface of the Earth. Thus, many of the world's national space agencies have sent missions to explore these bodies for scientific and other purposes.

These motivations have also led to the extensive study of spacecraft orbital dynamics in the proximity of these small bodies. In all asteroid rendezvous missions to date, the asteroids - though small - have been massive enough to require the attraction of these bodies to be taken into account. Previous missions have either orbited these bodies or have used propulsive controls to hover in their vicinity, essentially nulling the attraction of the asteroid on average. In this paper, we consider a possible future situation where the size of the target asteroid is so small, or the distance of the spacecraft from the asteroid large enough, to enable the overall attraction of the asteroid to be neglected.

There are several situations where such a target asteroid, or such a proximity dynamics, may fit the overall mission goals. A short discussion of them follows. First, if the target asteroid is quite small, on the order of tens of meters, it may be impossible for a spacecraft to enter direct orbit about it, but instead will be on a neighboring elliptic orbit about the sun, perhaps with some perturbation from the small asteroid mass. The discussion in this paper will show that this motion can be designed to stay on the sunward side of the

asteroid, and can vary periodically with an orbit period of one asteroid year. By adjusting the total acceleration acting on the spacecraft, it is also possible to place the spacecraft in an equilibrium point at an arbitrary point distance from a small asteroid on the sunward side. Also, if the asteroid is larger, a spacecraft can still be placed on a similar orbit that does not interact strongly with the asteroid an instead follows a neighboring heliocentric orbit that remains in the vicinity of the asteroid. Such a vantage point may allow for long-term monitoring of the asteroid, serve as a way-station for storing material to be used in the exploration of that asteroid, or if its instruments are properly designed may even be able to carry out substantive observations of the body. These are just some simple examples for when the situation studied in this paper could be of interest.

　　The paper is structured as follows. First the fundamental models for motion of a spacecraft about an asteroid are reviewed, along with the appropriate equations of motion. Then we consider situations where the attraction of the asteroid can either be neglected or relegated to a higher-order perturbation. The governing equations of motion are derived for these cases and their general solution discussed. Finally, we make some application of these equations and discuss situations where this model of motion could be used.

1　Asteroid and Spacecraft Model

　　We assume the asteroid has a heliocentric orbit defined by a semi-major axis a, eccentricity e and related orbit parameter p. Furthermore, we assume it has a mean radius of R and a bulk density of ρ, giving it a total mass of $M = 4\pi\rho R^3/3$ and a gravitational parameter of $\mu = GM$, where $G = 6.672\,4 \times 10^{-20}$ km³/s²/kg is the gravitational constant. In this paper and analysis we assume that the asteroid is spherical with constant density. We note that the shape of the body can have a dramatic effect on proximity orbital dynamics, as studied in [1], however we do not consider such complexities here. Thus the gravitational attraction of the asteroid is simply $-\mu r/r^3$, where r is the relative position vector of a point relative to the center of the asteroid and r denotes its magnitude.

　　The other significant perturbation we consider is

from the sun, both its gravitational attraction (modeled as a point mass with $\mu_{\text{Sun}} = 1.327 \times 10^{11}$ km³/s²), and due to the solar photons that impinge on the spacecraft. As a simple model we use the one presented in [1], which gives the solar radiation pressure acting on a spacecraft to be

$$a_{\text{SRP}} \sim \frac{(1 + \sigma)P_0}{B\,d^3}\,d \qquad (1)$$

where P_0 is a solar constant approximately equal to 1×10^8 kg km³/s²/m², d is the vector from the sun to the small body, σ is the reflectance of the spacecraft and B is the mass to area ratio of the spacecraft (in kg/m²) which controls the relative strength of this perturbation. Typical values of B range between $10 \sim 100$ kg/m². Although the solar photons also have an effect on the asteroid orbit, we note that it is quite small relative to the spacecraft, and thus is neglected herein.

2　Equations of Motion

2.1　Asteroid-Sun Relative Equations of Motion

　　The derivation of the equations of motion of a spacecraft in the vicinity of an asteroid, which in turn is in orbit about the sun, is derived in [1]. The most relevant form of these equations for analytical study are taken such that the fundamental frame rotates with the sun-asteroid line, making that a fixed axis of the system. If the asteroid's true anomaly about the sun and its time rate of change is represented as f and $\dot{f}$, then the equations of motion in this rotating frame are given as

$$\ddot{r} + 2\dot{f}\hat{z} \times \dot{r} + \ddot{f}\hat{z} \times r + \dot{f}^2\hat{z} \times \hat{z} \times r =$$
$$-\frac{\mu}{r^3}r + a_{\text{SRP}}\hat{d} + \frac{\mu_{\text{Sun}}}{d^3}\left[3\hat{d}\hat{d} \cdot r - r\right] \qquad (2)$$

where r is the position vector of the spacecraft, $\hat{d}$ is the unit vector pointing from the sun to the asteroid, and $\hat{z}$ is the direction perpendicular to the asteroid heliocentric orbit plane, and is the axis about which this frame rotates.

2.2　Scaled Equations of Motion

　　A standard approach for simplifying these equations is to introduce the true anomaly as an independent parameter and to scale the position vector by the time-varying distance $d = p/(1 + e\cos f)$, defining a new position vector $R = r/d$. Applying this transformation simplifies the equations of motion to

$$\boldsymbol{R}'' + 2\hat{\boldsymbol{z}} \times \boldsymbol{R}' + \hat{\boldsymbol{z}}\hat{\boldsymbol{z}} \cdot \boldsymbol{R}' =$$

$$\frac{1}{1 + e\cos f}\left[- \frac{\mu}{\mu_{\mathrm{Sun}}}\frac{\boldsymbol{R}}{R^3} + \beta\hat{\boldsymbol{d}} + 3\hat{\boldsymbol{d}}\hat{\boldsymbol{d}} \cdot \boldsymbol{R} \right] \qquad (3)$$

where $()'$ represents a derivative with respect to true anomaly (the new independent variable), the vector $\boldsymbol{R}$ is dimensionless and $\beta = \dfrac{(1 + \sigma)P_0}{\mu_{\mathrm{Sun}}B}$ is a non-dimensional term that represents the strength of the SRP force in terms of local solar gravitational attraction. Rewriting the equations in scalar form (assuming that $\hat{\boldsymbol{d}} = \hat{\boldsymbol{x}}$) yields

$$X'' - 2Y' = \frac{1}{1 + e\cos f}\left[- \frac{\mu}{\mu_{\mathrm{Sun}}}\frac{X}{R^3} + \beta + 3X \right] \qquad (4)$$

$$Y'' + 2X' = \frac{1}{1 + e\cos f}\left[- \frac{\mu}{\mu_{\mathrm{Sun}}}\frac{Y}{R^3} \right] \qquad (5)$$

$$Z'' + Z = \frac{1}{1 + e\cos f}\left[- \frac{\mu}{\mu_{\mathrm{Sun}}}\frac{Z}{R^3} \right] \qquad (6)$$

This equation was studied in [2] in a slightly different form. These equations have a close affinity with the elliptic restricted 3-body problem, with the change of moving the origin to the smaller primary, the addition of Hill's approximation for the effect of the larger primary, and the effect of the solar radiation pressure.

Given a solution to these equations, as a function of true anomaly f, it can be scaled back to a fully dimensional solution relative to the asteroid center as

$$\boldsymbol{r} = d\boldsymbol{R} \qquad (7)$$

$$\dot{\boldsymbol{r}} = \sqrt{\frac{\mu_{\mathrm{Sun}}}{p}}\,e\sin f\boldsymbol{R} + \sqrt{\frac{\mu_{\mathrm{Sun}}}{p}}\,(1 + e\cos f)\boldsymbol{R}' \qquad (8)$$

2.2.1 Parameter Values

For the current study it is reasonable to evaluate representative values for the parameters β and μ/μ_{Sun}. For β, we set $\sigma = 0$ for convenience and leave B unspecified, to find

$$\beta = 7.5 \times 10^{-4}/B \qquad (9)$$

where B is given in units of kg/m². Across our range of B values we see that $\beta = 7.5 \times 10^{-5} \rightarrow 7.5 \times 10^{-6}$.

For the ratio of the asteroid and solar GM, we leave the asteroid density and radius as free parameters. This provides us with

$$\frac{\mu}{\mu_{\mathrm{Sun}}} = 2.1 \times 10^{-30}\rho R^3 \qquad (10)$$

where ρ is in kg/m³ and R is in m. While we see that the magnitudes of these two non-dimensional parameters are quite different, we shall see next that when appropriately balanced they yield reasonable values.

Finally, we note that for definiteness when necessary we assume the asteroid is at approximately 1 AU or $\sim 1.5 \times 10^8$ km.

2.2.2 Limits for Gravitational Influence

The current study is specifically interested in when the attraction of the central asteroid can be neglected, as an approximation. To analyze this we leverage our previous study of these equations and the modified Hill sphere about the asteroid, accounting for SRP on the spacecraft. The limits of the Hill sphere can be approximately defined as the distance of the relative equilibria from the asteroid center. If the SRP effect is ignored, this results in the well-known equilibrium points for the Hill problem

$$x_{\pm}^* = \pm d\left(\frac{\mu}{3\mu_{\mathrm{Sun}}} \right)^{1/3} = \pm 13.3\rho^{1/3}RD \qquad (11)$$

where D is the distance in AU and with $y^* = z^* = 0$. For a typical density of $2\,000$ kg/m³ this distance becomes about 168 times the asteroid radius at 1AU.

We are more interested in the case when the SRP acceleration is large compared to the gravitational attraction of the asteroid. We can formally represent this case as $\beta >> \mu/\mu_{\mathrm{Sun}}/R^2$. Then (as studied in more detail in [1~2]) the two equilibrium points become different in distance from the asteroid, with the sunward side ($X < 0$) getting relatively far from the body and the anti-sunward side ($X > 0$) getting very close to the body. At lowest order, the sunward side equilibrium distance is

$$x_{-}^* \sim - \frac{d}{3}\beta = 3.75 \times 10^4 D/B \text{ km} \qquad (12)$$

with $y^* = z^* = 0$ again. For a mass to area ratio of 100 kg/m² this is 375 km away from the body towards the sun. Note that this point is, to first order, independent of the asteroid gravitational attraction.

The anti-sunward side equilibrium distance is

$$x_{+}^* \sim d\sqrt{\frac{\mu}{\mu_{\mathrm{Sun}}\beta}} = 7.9 \times 10^{-6}\sqrt{\rho R^3 B} \text{ km} \qquad (13)$$

with $y^* = z^* = 0$ again. Thus for our typical case of $\rho =$

2 000 kg/m³ and $B = 100$ kg/m² this is a distance of $3.5 \times 10^{-3} R^{3/2}$ km. When closer to the asteroid than this distance, the object can sustain orbit about it for at least a limited time. We see that this equilibrium point will be at or below the surface of the asteroid when $R \leqslant 17$ m in size. Even for larger asteroids we note that this distance is relatively small compared to the sunward equilibrium point.

2.3 Approximate Equations of Motion

In the following we will formalize our assumption on the relative smallness of the asteroid gravity by introducing the parameter $\varepsilon = \mu/\mu_{Sun}$. The solution will be expanded by analytic continuation in this term as $\boldsymbol{R} = \boldsymbol{R}_0 + \varepsilon \boldsymbol{R}_1 + \varepsilon^2 \boldsymbol{R}_2 + \ldots$ following standard techniques[3]. Applying this expansion we find the zeroth order differential equations to be

$$X''_0 - 2Y'_0 = \frac{1}{1 + e\cos f}\left[\beta + 3X_0\right] \quad (14)$$

$$Y''_0 + 2X'_0 = 0 \quad (15)$$

$$Z''_0 + Z_0 = 0 \quad (16)$$

This is a modified form of the Tschauner-Hempel (TH) equations, which represent linearized motion about an elliptic orbit[4-6]. The TH equations can be solved in closed form, and we show that this version of them can also be solved with the same technique. A spacecraft's trajectory avoiding close approaches to the central asteroid would follow these equations.

The differential equations for the first order solution can be derived to be

$$X''_1 - 2Y'_1 = \frac{1}{1 + e\cos f}\left[3X_1 - \frac{X_0}{R_0^3}\right] \quad (17)$$

$$Y''_1 + 2X'_1 = -\frac{1}{1 + e\cos f}\frac{Y_0}{R_0^3} \quad (18)$$

$$Z''_1 + Z_1 = -\frac{1}{1 + e\cos f}\frac{Z_0}{R_0^3} \quad (19)$$

These are again a perturbed variation of the Tschauner-Hempel equations, with a non-homogeneous term driven by the solution of the zeroth order equations. The equations of motion for higher-order variations will have the same linear structure as above, but increasingly complex expansions of the lower order solutions.

3 Solutions to the Equations

In the following we detail the solution to the zeroth order equations of motion and give the form of the solution for higher-order effects.

3.1 Zeroth Order Equations

If we make the substitution $\bar{X}_0 = X_0 + \frac{1}{3}\beta$, the equations fall into the standard TH form, displacing the center towards the sun by the nominal equilibrium point distance.

$$\bar{X}''_0 - 2Y'_0 = \frac{1}{1 + e\cos f}3\bar{X}_0 \quad (20)$$

$$Y''_0 + 2\bar{X}'_0 = 0 \quad (21)$$

$$Z''_0 + Z_0 = 0 \quad (22)$$

Then the solution can be expressed in standard form. In the following we rely on the discussion by [5], who gives a thorough review of the solutions to the TH equations.

Define a state vector as $\bar{\Xi}_0 = \left[\bar{X}_0, Y_0, Z_0, X'_0, Y'_0, Z'_0\right]$. Then the general orbit solution can be specified as a linear mapping

$$\bar{\Xi}_0 = \boldsymbol{\Phi}(f, f_o)\bar{\Xi}_o \quad (23)$$

where $\boldsymbol{\Phi} \in \boldsymbol{R}^{6 \times 6}$ is the state transition matrix for the system. The entries of $\boldsymbol{\Phi}$ can be written out in detail as

$$\boldsymbol{\Phi} = \begin{bmatrix} \varphi_{XX} & \varphi_{XY} & 0 & \varphi_{XX'} & \varphi_{XY'} & 0 \\ \varphi_{YX} & \varphi_{YY} & 0 & \varphi_{YX'} & \varphi_{YY'} & 0 \\ 0 & 0 & \varphi_{ZZ} & 0 & 0 & \varphi_{ZZ'} \\ \varphi_{X'X} & \varphi_{X'Y} & 0 & \varphi_{X'X'} & \varphi_{X'Y'} & 0 \\ \varphi_{Y'X} & \varphi_{Y'Y} & 0 & \varphi_{Y'X'} & \varphi_{Y'Y'} & 0 \\ 0 & 0 & \varphi_{Z'Z} & 0 & 0 & \varphi_{Z'Z'} \end{bmatrix} \quad (24)$$

where we inserted zeros in all of the cross coupling terms between the out-of-plane and in-plane terms. The remaining terms are then, taking $f_o = 0$,

$$\varphi_{XX} = \frac{1}{1 - e}\left[4 + 2e - 3\cos f - 3e\cos^2 f - 3e(2 + e)\sin f(1 + e\cos f)L\right] \quad (25)$$

$$\varphi_{XY} = 0 \quad (26)$$

$$\varphi_{XX'} = \frac{1}{1 + e}\sin f(1 + e\cos f) \quad (27)$$

$$\varphi_{XY'} = \frac{1}{1 - e}\left[2 + 2e - 2\cos f - 2e\cos^2 f - 3e(1 + e)\sin f(1 + e\cos f)L\right] \quad (28)$$

$$\varphi_{YX} = \frac{1}{1-e}\big[3\sin f\,(2 + e\cos f\,)$$
$$-3(2 + e\,)(1 + e\cos f\,)^2 L\big]$$

$$\varphi_{YY} = 1 \qquad (29)$$

$$\varphi_{YX'} = \frac{1}{1+e}\big[\cos f\,(2 + e\cos f\,) - (2 + e\,)\big]$$

$$\varphi_{YY'} = \frac{1}{1-e}\big[2\sin f\,(2 + e\cos f\,) -$$
$$3(1 + e\,)(1 + e\cos f\,)^2 L\big] \qquad (30)$$

$$\varphi_{X'X} = \frac{1}{1-e}\big[\,3\sin f + 3e\sin 2f -$$
$$3e(2 + e\,)(\cos f + e\cos 2f\,)L - \frac{3e(2 + e\,)\sin f}{1 + e\cos f}\,\big] \qquad (31)$$

$$\varphi_{X'Y} = 0 \qquad (32)$$

$$\varphi_{X'X'} = \frac{1}{1+e}\big[\cos f + e\cos 2f\,\big] \qquad (33)$$

$$\varphi_{X'Y'} = \frac{1}{1-e}\,\big[\,2\sin f + 2e\sin 2f -$$
$$3e(1 + e\,)(\cos f + e\cos 2f\,)L - \frac{3e(1 + e\,)\sin f}{1 + e\cos f}\,\big] \qquad (34)$$

$$\varphi_{Y'X} = \frac{1}{1-e}\,\big[\,6\cos f + 3e\cos 2f$$
$$-3(2 + e\,)(1 - 2e\sin f\,(1 + e\cos f\,)L\,)\big] \qquad (35)$$

$$\varphi_{Y'Y} = 0 \qquad (36)$$

$$\varphi_{Y'X'} = \frac{-2\sin f\,(1 + e\cos f\,)}{1 + e} \qquad (37)$$

$$\varphi_{Y'Y'} = \frac{1}{1-e}\,\big[\,4\cos f + 2e\cos 2f -$$
$$3(1 + e\,)(1 - 2e\sin f\,(1 + e\cos f\,)L\,)\big] \qquad (38)$$

$$\varphi_{ZZ} = \cos f \qquad (39)$$

$$\varphi_{ZZ'} = \sin f \qquad (40)$$

$$\varphi_{Z'Z} = -\sin f \qquad (41)$$

$$\varphi_{Z'Z'} = \cos f \qquad (42)$$

where we note the function L is defined as

$$L(f\,) = \int \frac{\mathrm{d}f}{(1 + e\cos f\,)^2} = \sqrt{\frac{\mu}{p^3}}\,t \qquad (43)$$

where t is the time from perihelion. Thus we see that L will linearly increase in time, and could lead to a secular drift between the spacecraft and the asteroid.

3.2 Linear Drift in Orbit

It is instructive if we combine all terms that contain the drift term L, as in general we would like to eliminate this term on average. This is most easily seen if we combine the different solution components as

$$X = -3e\sin f\,(1 + e\cos f\,)\big[\,(2 + e\,)X_o +$$
$$(1 + e\,)Y'_o\big]L + \dots \qquad (44)$$

$$Y = -3(1 + e\cos f\,)^2\big[\,(2 + e\,)X_o +$$
$$(1 + e\,)Y'_o\big]L + \dots \qquad (45)$$

$$X' = -3e(\cos f + e\cos 2f\,)\big[\,(2 + e\,)X_o +$$
$$(1 + e\,)Y'_o\big] + \dots \qquad (46)$$

$$Y' = 6e\sin f\,(1 + e\cos f\,)\big[\,(2 + e\,)X_o +$$
$$(1 + e\,)Y'_o\big] + \dots \qquad (47)$$

It is significant to note that the drift appears in the X, X' and Y' components as well, a situation that does not occur for the circular orbit case.

It is simple to see that all of the drift terms involve the combination of initial conditions $(2 + e\,)X_o + (1 + e\,)Y'_o$, and thus choosing this combination to be zero will ensure that the drift terms do not appear. The simplest way to ensure this is to choose

$$Y'_o = -\frac{2 + e}{1 + e}X_o \qquad (48)$$

Substituting these initial conditions into the solutions for X and Y we find

$$X = \frac{1}{1+e}\,\{\,\cos f\,(1 + e\cos f)X_o +$$
$$\sin f\,(1 + e\cos f)X'_o\} \qquad (49)$$

$$Y = Y_o - \frac{1}{1+e}\,\{\,\sin f\,(2 + e\cos f\,)X_o -$$
$$\big[\cos f\,(2 + e\cos f\,) - (2 + e\,)\big]X'_o\} \qquad (50)$$

To get a better sense of the geometry of motion, we can put these equations into the general form of an ellipse. Doing so then yields the parametric equation

$$1 = \frac{(1+e)^2}{X_o^2 + X_o'^2}\left\{\left(\frac{X}{1 + e\cos f}\right)^2 + \left(\frac{Y - Y_o + \dfrac{2+e}{1+e}X_o'}{2 + e\cos f}\right)^2\right\} \qquad (51)$$

From this equation we see that the path of the spacecraft will follow an "osculating" ellipse that is centered at $X = 0$ and $Y = Y_o - \dfrac{2+e}{1+e}X'_o$ with a pulsating "size" along the X axis equal to $\dfrac{1 + e\cos f}{1 + e}\sqrt{X_o^2 + X_o'^2}$, and along the Y axis equal to $\dfrac{2 + e\cos f}{1 + e}\sqrt{X_o^2 + X_o'^2}$. We note that the relative extent of these directions is now $(1 + e\cos f\,)/(2 + e\cos f\,)$, and

varies from $(1 + e)/(2 + e) \rightarrow (1 - e)/(2 - e)$ within one heliocentric orbit of the asteroid. When the drift term is nulled out we see that the resulting motion is stable.

Figure 1 shows this relative bounded motion in the scaled coordinates over one heliocentric period for a number of different asteroid eccentricities, for a trajectory chosen in the asteroid orbital plane. Here, at periapsis the spacecraft is at a fixed location along the $-X$ axis, which runs vertical. For increasing eccentricity the relative motion deviates strongly from an ellipse. Recall that the asteroid is located at the coordinate $\beta/3$ along the X axis (in scaled coordinates), so that depending on the strength of the SRP, the entire relative trajectory may lie on the sunward side of the asteroid.
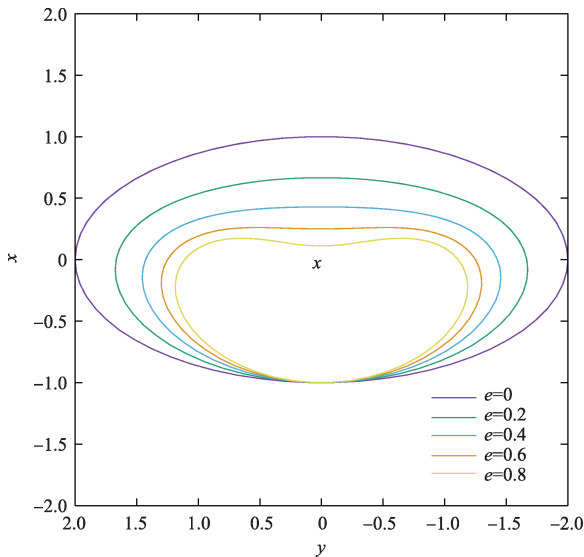

Fig. 1　Bounded motion zeroth order scaled solution for different asteroid eccentricities. The X axis points up and away from the sun and the Y axis to the left along the direction of asteroid motion，following usual convention for the Clohessy-Wiltshire equations. The asteroid will lie at a value $X = \beta/3$ measured from the origin on the plot

3.3　Higher Order Corrections

For solving the first order corrections we note that the linear part of the equations are satisfied by the state transition matrix $\boldsymbol{\Phi}$ introduced above. The zeroth order solutions have the form

$$\Xi_0 = \boldsymbol{\Phi}(f,f_o)\bar{\Xi}_o - \frac{1}{3}\beta\begin{bmatrix}1\\0\\0\\0\\0\\0\end{bmatrix} \qquad (52)$$

and this solution is substituted into the first order

equations of motion given in Eqns. 17～19. We note that the state transition matrix $\boldsymbol{\Phi}(f,f_o)$ is computed from the form given in Eqn. 24, $\boldsymbol{\Phi}(f,0)$, as $\boldsymbol{\Phi}(f,f_o) = \boldsymbol{\Phi}(f,0)\boldsymbol{\Phi}^{-1}(f_o,0) = \boldsymbol{\Phi}(f,0)\boldsymbol{\Phi}(0,f_o)$.

Applying standard variation of constants for non-homogeneous linear systems we can then express the first order correction as

$$\Xi_1 = \boldsymbol{\Phi}(f,f_o)\!\int_{f_o}^{f}\boldsymbol{\Phi}^{-1}(f',f_o)\begin{bmatrix}0\\B\end{bmatrix}df' \qquad (53)$$

where 0 is a 3×1 zero vector and

$$B = -\frac{1}{1 + e\cos f}\begin{bmatrix}\dfrac{X_0}{R_0^3}\\[6pt]\dfrac{Y_0}{R_0^3}\\[6pt]\dfrac{Z_0}{R_0^3}\end{bmatrix} \qquad (54)$$

where the nominal linear solution is substituted into X_0, Y_0 and Z_0, and combined together into $R_0 = \sqrt{X_0^2 + Y_0^2 + Z_0^2}$. Higher order solutions can be generated in much the same way, providing a rigorous approach to developing an analytical solution to the full equations of motion.

With this correction term, the full solution to first order is then

$$\Xi = \boldsymbol{\Phi}(f,f_o)\bar{\Xi}_o - \frac{1}{3}\beta\begin{bmatrix}1\\0\\0\\0\\0\\0\end{bmatrix} + \varepsilon\Xi_1(f,f_o) \qquad (55)$$

We note that this form of the equations holds for both circular and elliptic cases.

As a specific example we consider the equilibrium point solution for the circular orbit case. Then the zeroth order state solution is, identically, $\Xi_0 = \left[-\frac{1}{3}\beta,0,0,0,0,0\right]$. The correction term is

$$\Xi_1 = \frac{1}{(\beta/3)^2}\begin{bmatrix}1 - \cos f\\2\sin f\\0\\\sin f\\\cos f - 1\\0\end{bmatrix} \qquad (56)$$

and the full expression for the time-varying in-plane positions are

$$X = -\frac{1}{3}\beta + \frac{\varepsilon}{(\beta/3)^2}(1 - \cos f) \quad (57)$$

$$Y = 2\frac{\varepsilon}{(\beta/3)^2}\sin f \quad (58)$$

4 Discussion

We finish this paper by discussing how these equations and their solution can be used in developing mission designs to small asteroids or that keep a far distance to the central asteroid. The most significant aspect to consider is the existence of the sunward equilibrium point, which serves as a natural vantage point for observation. In these linear equations the equilibrium point is technically unstable, as a small random error will excite the drift term and cause the spacecraft to drift away from the body at a linear increase in time. This instability is not exponential, and thus it can be easily nulled through the execution of control maneuvers. The influence of the asteroid gravitational attraction is seen to only cause an oscillation in its location and, in some sense, stabilizes the motion. Note that the full stability of these equilibria are considered in [2]. It is also significant to note that the location of this equilibrium point can be controlled by the addition of a small amount of thrusting. If a constant thrust is added towards the sun, the effect of the SRP is reduced and the equilibrium point will move towards the asteroid. Conversely, thrusting away from the sun will push the equilibrium further from the asteroid and towards the sun. As the level of thrusting is less than the effect of SRP on the spacecraft, we see that by definition this is a modest thrust.

In addition to the stationary equilibrium orbits, it is also possible to utilize the time-varying periodic solutions. These will naturally provide a range of viewing geometries, and can also be excited in the out of plane direction. These orbits can be chosen such that they always remain on the sunward side, or if a larger amplitude is used can also cross the asteroid radius and pass behind the asteroid. A drawback for these orbits is their long period, an asteroid year. Thus, they may only be of interest for long-term monitoring or a mission with no significant time constraints. Again, it is possible to modify the characteristics of these orbits through the addition of a small value of thrust towards or away from the sun.

The current discussion does not consider the first order perturbations to these solutions except in the most trivial case. A future topic of interest would be what the effect of the asteroid gravity is, at first order, when the spacecraft is parked at a distance away from the sun-asteroid line or when it is placed into a periodic orbit. These cases can all be considered rigorously as the general solution to the equations is known, and the first order perturbations can be evaluated through a simple quadrature.

5 Conclusion

This paper considers the orbital dynamics and design of trajectories about very small asteroids or distant from larger asteroids. In these cases the motion is dominated by the heliocentric asteroid orbit, and motion occurs on a timescale of one asteroid year. Despite this drawback, there may be specific applications that may be attractive in these situations, and which this analysis may help develop. The paper provides a summary of the equations governing spacecraft motion in this case and reviews the basic solution procedures for these equations.

References

[1] SCHEERESD J. Orbital motion in strongly perturbed environments: applications to asteroid, comet and planetary satellite orbiters[M]. London (UK): SpringerPraxis, 2012.

[2] SCHEERESD J, MARZARI F. Spacecraft dynamics far from a comet [J].The Journal of the Astronautical Sciences, 2002, 50(1): 35-52.

[3] MOULTONF R. Differential equations [M]. UK: The MacMillan Company, 1930.

[4] THOMAS E C. New form for the optimal rendezvous equations near akeplerian orbit [J]. Journal of Guidance, Control, and Dynamics, 1990, 13(1):183-186.

[5] DANG Z H. Solutions of tschauner-hempel equation [J]. Journal ofGuidance, Control, and Dynamics, 2017, 40(11): 2956-2960.

[6] YAMANAKA K, ANKERSEN F. New state transition matrix for relative motion on an arbitrary elliptical orbit[J]. Journal of Guidance, Control, and Dynamics, 2002, 25(1): 60-66.

作者简介：

丹尼尔 J. 谢尔斯（1963-），男，美国科罗拉多大学巨石分校教授，主要研究方向：宇航动力学、卫星导航。

通讯地址：429 UCB, Boulder, CO 80309-0429, USA

电话：(720) 544-1260

E-mail: scheeres@colorado.edu

小行星远距离抵近轨道

丹尼尔 J. 谢尔斯

（科罗拉多大学 博尔德分校 史密德航天工程科学系，博尔德 80309-0429，美国）

摘　要：讨论了小行星引力一阶项可被忽略情况下的小行星远距离轨道设计及动力学。此时，航天器的运动受太阳引力和太阳光压的影响。航天器和小行星的加速度之差在这两者之间形成的独特的相对动力学，为航天器在小行星附近停驻与观测提供特定轨道。完整解决了小行星处于圆形日心轨道这一较简单情况，也考虑和阐述了椭圆轨道情况，并取得了一些初步结果。

关键词：小行星；抵近轨道；运动方程；高阶校正

[责任编辑：高莎]

The Development Overview of Asteroid Exploration

ZHANG Rongqiao[1]，HUANG Jiangchuan[2]，HE Rongwei[2]，GEN Yan[1]，MENG Linzhi[3]

（1. Lunar Exploration and Aerospace Engineering Center，Beijing 100190；
2. China Academy of Space Technology，Beijing 100094；
3. Beijing Institute of Spacecraft System Engineering，Beijing 100094）

Abstract：The small bodies retain the original elements of early solar system，and may contain important clues to the origin of the earth's life and water. They are living fossils for studying the origin and evolutionary history of the solar system. Asteroid exploration has become research hotspots of international deep space exploration in recent years. The process of small bodies exploration is briefly summarized，and the research and development of asteroid exploration is reviewed，as well the key technologies of asteroid missions. Based on the deep space exploration capability of China， some suggestions are put forward to carry out future asteroid exploration.

Keywords：asteroid exploration；key technology；development overview

Highlights：
- The small bodies retain the original elements of early solar system，and they are living fossils for studying the origin and evolutionary history of the solar system.
- Asteroid exploration has become research hotspots of international deep space exploration in recent years.
- The research and development status of asteroid exploration is summarized and reviewed.
- The key technologies of asteroid exploration missions are analyzed.

[责任编辑：高莎，英文审校：朱恬]